Mathematical analysis of in-host Ebola virus infection dynamics model with sensitivity analysis

Seleman Ismail[*]

The Open University of Tanzania, PO Box 23409, Dar es Salaam, Tanzania

ABSTRACT

Ebola virus (EBOV) causes a haemorrhagic and lethal Ebola disease disastrous to human beings, which is transmitted by contact of body fluids of infected animals and humans. Presently, there are no therapies for the disease. In this paper, a mathematical model is proposed to investigate the in-vivo dynamics of EBOV infection with sensitivity analysis. A system of five non-linear ordinary differential equations constitutes the model, from which the basic reproduction number, R_0 is calculated using the next generation matrix method. The parameter R_0 is employed to analyze global stability of disease-free and endemic equilibria. Using the Metzler matrix operator, the results indicate that the disease-free equilibrium point is globally asymptotically stable provided that $R_0 < 1$, which implies that the disease disappears from the host after some period of time. With Lyapunov Stability Theory and LaSalle Invariant Principle, the results indicate that the endemic equilibrium point is globally asymptotically stable provided that $R_0 > 1$, which implies that the disease persists in the host. Sensitivity analysis of the basic reproduction number pertaining to the model parameters is achieved using forward normalized sensitivity index method. The results indicate that the parameters for infection rate, production rate of uninfected target cells and virus replication rate are positively sensitive. On the other hand, the parameters for natural death rate of target cells and natural death rate of the virus are negatively sensitive, implying that the basic reproduction number decreases as the parameters increase and vice versa. Besides, it is shown that the parameter for the infection rate is the most sensitive one while the parameter for the virus reproduction rate is the least sensitive one. Numerical simulations are used to validate the analytical results. The results suggest implementation of deliberate control measures to eradicate EBOV disease by considering sites in the model to which the most sensitive parameters are affiliated.

Keywords: EBOV model; Basic reproduction number; Global stability; Sensitivity analysis*; Antibody response.*

INTRODUCTION

Ebola virus (EBOV) is a single-stranded negative-sense RNA virus, which belongs to the family Filoviridae, from Latin word *filum* which means *thread* (Carter and Sounders, 2013). EBOV was first known in 1976 near Ebola River found in the

---

[*] Corresponding author: selemanismail@yahoo.com

Democratic Republic of Congo (DRC) (Fritz, 2012; ECDC, 2022). EBOV is classified in five strains known as Zaire, Tai Forest (Ivory Coast), Sudan, Bundibugyo and Reston strains. Of the five strains, Zaire and Sudan strains have largely caused human Ebola diseases. The virus causes dreadful hemorrhagic and lethal Ebola virus disease (EVD) to humans. Ever since it was known, several EVD outbreaks amongst humans have occurred sporadically in several Sub-Saharan countries, mostly in Gabon, South Sudan, Ivory Coast, Uganda and South Africa (CDC, 2014). EBOV was the source of the 2013-2015 EVD outbreak, the largest ever in history, in some West African countries, which resulted in at least 230114 total cases and 9840 total deaths as of March 4, 2015 (CDC, 2015). About 14 EVD outbreaks have been recorded in DRC since 1976 and the most recent one occurred in 2022 (IFRC, 2022). The 2018-2020 outbreak was the second largest in history, which resulted in a total of 3481 cases, 1162 recoveries and 2299 deaths (WHO, 2021). Recently, an outbreak of EVD was reported in Uganda, where seven cases were confirmed to have contracted Sudan ebolavirus, including one death; forty-three identified and ten people suspected to have been infected with the virus were getting treatment at Mubende Regional Hospital as of September 22, 2022 (WHO, 2022). WHO also reported 131 confirmed cases of EVD, including 48 deaths, as of November 2, 2022. There are no licensed vaccines against EVD caused by Sudan ebolavirus

Overall, EVD has been a world tragedy to human health as it jeopardizes human health because of its hemorrhagic and lethal nature. The disease can cause death to an infected host in less than two days (Peters, 1999). EBOV can be transmitted from animal to animal, human to human and animal to human. Humans can be infected through saliva, mucus, vomit, faeces, sweat, tears, breast milk, urine and semen of infected individuals. The symptoms of the disease, EVD, are typically headache, fever, vomiting, bleeding, diarrhea and rash (Fauci, 2014). The chance of death from the disease is about 60% and upsurges as the disease progresses to hemorrhagic stage. Currently, there is no cure for EVD (Melinda, 2022). Nevertheless, the virus transmission and subsequent deaths can be largely reduced through early detection and effective contact tracing (Beeching *et al.,* 2014). Symptomatic infected individuals are usually supported by maintaining fluids, electrolytes and acid-base balance of blood and treating secondary infections (Tseng and Chan, 2015).

Ahead of model formulation, it is necessary to understand how the immune system functions in response to EBOV infection. This is because survival from EVD is governed by the host's ability to develop and manifest a robust immune response early after the virus infection (Wester, 2015). A major element of the immune system is the T-cell, which is a lymphocyte that develops in the thymus. The T-cells usually exist in two different cells populations: Helper T-cells or CD4 and Cytotoxic T lymphocytes (CTL) or CD8. The acronyms CD4 and CD8 represent classes of

proteins on the surface of these cells. (Nowak and May, 2000; Wodarz, 2005; Ramirez, 2014) Once the virus is introduced into the host's body, the T-cells become activated, which is the launch of an adaptive immune response (Roemer, 2013; Wester, 2015). The activated T-cells discharge cytokines and proliferate. The cytokines are a chemical mediator that functions as the communication coordination for the immune system. Moreover, the cytokines, discharged by Helper T-cells, largely contribute to the activation and proliferation of CTLs. When the CTLs are exposed to the cytokines discharged by the activated Helper T-cell, they themselves become activated (Rihan *et al*., 2013; Wester, 2015). The T Helper cells also play an important role in the activation of the B-cells and so in the discharge of antibodies. The B-cells release antibodies that deactivate free viruses. The moment the CTLs are activated, they start generating chemicals that kill infected cells. The infected cells become a factory of production of new viruses (Ramirez, 2014). Activation of CTLs is indispensable in investigating the stimulation and effect of the CTL when investigating the course of infection. The CTL response is a major element of host survival and regaining during a viral infection; this is because of its ability to kill infected cells on contact (Wester, 2015). This study aims at investigating the role of the CTLs and antibody responses in the dynamics of in-host EBOV infection.

Mathematical modeling has been an important tool in Mathematical Epidemiology. It has been used to forecast transmission and extinction of an infectious disease as time elapses (Okosun and Makinde, 2014; Osman and Makinde, 2018; Eyaran *et al*., 2019; Osman *et al*., 2020e; Onsongo *et al*., 2022). It has been contributory in investigating mechanisms that govern viral kinetics in order to provide a quantitative understanding and formulate recommendations for treatments (Nguyen, 2015). Modeling involves the following important aspects: formulation of a model and checking it for biological legitimacy, analysis of the model, where the model equilibria and basic reproductive number are obtained; stability analysis of the model equilibria; sensitivity analysis, which helps to identify locations in the model where deliberate efforts can be directed in order to control the course of infection. Moreover, it functions as a platform for implementing an optimal control strategy, which is anticipated to provide plausible methodologies for disease control and eradication. As yet, few models have been formulated to investigate in-host dynamics of EBOV. Wester (2015) developed a model to investigate in-vivo dynamics of EBOV with the CTL response, whereby stabilities of the model equilibria were analyzed and the results indicated that they are locally and globally asymptotically stable. Ismail and Mtunya (2021) protracted the model in order to study the dynamics of EBOV with suppressed CTL response by the virus. The study focused on sensitivity analysis of the threshold parameter R_0 with respect to the model parameters. The results indicated that the parameter for infection rate was the most sensitive one while the least sensitive parameter was the rate of viral reproduction. In the current study, the proposed model will involve all dynamical

effectors of the aforementioned models and antibody response. Then sensitivity analysis will be performed to investigate the influence of each model parameter on the threshold R_0, obtained from the model. Since there are no consistent therapies and vaccines, studies on the dynamics of Ebola infection and search of suitable control strategies are ongoing. Thus, findings of the current study provide the rationale for further investigation to understand the dynamics of EVD and stimulate more effective control strategies.

MATERIALS AND METHODS

Formulation of the model

The model is formulated based on the assumptions introduced by Ismail and Mtunya (2021)

a. Uninfected cells increase at a constant rate and have equal chances of being infected by the virus.
b. The uninfected and infected cells die naturally at equal constant rates. The infected cells produce viruses at a constant rate.
c. The viruses are produced from infected cells at a constant rate, die naturally at a constant rate and suppress (kill) cytotoxic T-lymphocytes at a constant rate.
d. The cytotoxic T-lymphocytes are produced, eliminate infected cells and die naturally at constant rates.
e. The antibody cells are produced at a constant rate and die naturally at constant rates.

The model consists of four heterogeneous populations, which are organized in six compartments: uninfected human target cells, infected human target cells, free Ebola virus (EBOV) population, cytotoxic T lymphocytes population and antibodies cells population. The variables $U(t)$, $I(t)$, $V(t)$, $Z(t)$ and $W(t)$ represent the numbers of populations at time t respectively. For simplicity of analyzes and discussions, the variables are condensed to U, I, V, Z and W, respectively. Uninfected cells, U are increased by a production rate Π and die naturally at the rate αU. Free viruses, V interact with the uninfected cells at the rate βVU to produce infected cells, I. The free viruses kill cytotoxic T lymphocytes, Z at the rate σVZ and die naturally at the rate ηV. The cytotoxic T lymphocytes increase at the rate λIZ, kill the infected cells at the rate πIZ and die naturally at the rate γZ. The infected cells replicate viruses at the rate ωI, which increases the virus population, and die naturally at the rate αI. The antibody cells, W increase at the rate εBW, kill the viruses at the rate μBW and die naturally at the rate ρW. The descriptions of the model parameters are presented in Table 1.

Table 1. Parameter Descriptions.

Parameter	Description
β	Infection rate of uninfected target cells.
α	Natural death rate of the uninfected and infected target cells.
γ	Natural death rate of cytotoxic T lymphocytes.
η	Natural death rate of the virus.
ρ	Natural death rate of antibodies.
μ	Extermination rate of the virus.
ε	Production rate of antibody cells.
ω	Replication rate of the virus.
λ	Production rate of cytotoxic T lymphocytes.
π	Extermination rate of infected cells.
σ	Suppression rate of cytotoxic T lymphocytes
Π	Production rate of uninfected target cells

Diagram of EBOV dynamics model

In view of the assumptions, descriptions of variables, parameters and dynamics, a diagram of Ebola virus dynamics model is presented, which is shown in Figure 1.
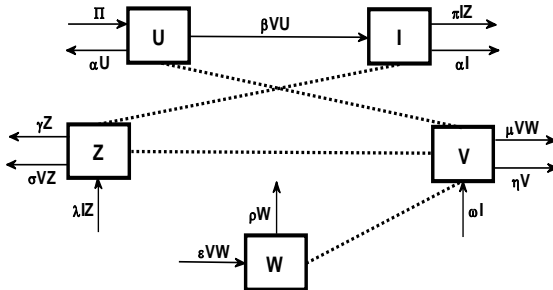

Figure 1. Diagram of EBOV dynamics model.

Equations of the model

In view of the descriptions of model state variables, parameters and dynamics, a system of five non-linear ordinary differential equations is formulated, where Equation 1 defines the dynamics of the uninfected target cells population; Equation 2, the infected cells population; Equation 3, the virus population; Equation 4, the CTLs population and Equation 5, the antibodies population.

$$\frac{dU}{dt} = \Pi - \beta VU - \alpha U \tag{1}$$

$$\frac{dI}{dt} = \beta VU - \pi IZ - \alpha Z \tag{2}$$

$$\frac{dV}{dt} = \omega I - \mu VW - \eta V \tag{3}$$

$$\frac{dZ}{dt} = \lambda IZ - \sigma VZ - \gamma Z \tag{4}$$

$$\frac{dW}{dt} = \varepsilon VW - \rho W \tag{5}$$

where $U(0) \geq 0$, $I(0) \geq 0$, $V(0) \geq 0$, $Z(0) \geq 0$ and $W(0) \geq 0$ are the given initial conditions.

Basic properties of the model

For biological validity of the model, the solutions to the system of equations $(1) - (5)$ must be positive and bounded for all values of time. For example, concluding that a virus population is negative is certainly unrealistic. Besides, the populations' sizes must be finite as the human body consists of a finite number of cells (Wester, 2015). The boundedness and positivity of solutions indicate that once an individual is infected, the virus population will remain below the detectable boundary without triggering significant impairment (Roemer, 2013). In consideration of this, proofs of positivity and boundedness for the system of equations $(1) - (5)$ are presented, which are achieved through Lemma 1 and Lemma 2, respectively.

Positivity of Solutions
Lemma 1: *Let* $t_0 > 0$. *If the initial conditions satisfy:* $U(0) \geq 0$, $I(0) \geq 0$, $V(0) \geq 0$, $Z(0) \geq 0$ and $W(0) \geq 0$, *then* $U(t)$, $I(t)$, $V(t)$, $Z(t)$ and $W(t)$ *will remain positive in* $R_+^5, \forall t \in [0, t_0]$.

Proof: At this point, it is required to prove that $U(t)$, $I(t)$, $V(t)$, $Z(t)$ and $W(t)$ will remain positive in $R_+^5, \forall t \in [0, t_0]$. It is known that all parameters used in the model are positive. Then, from the model system of equations $(1) - (5)$, a lower bound can be placed on each equation as shown below.

.

$$\left.\begin{array}{l} \dfrac{dU}{dt} \geq -\beta VU - \alpha U \\[2mm] \dfrac{dI}{dt} \geq -\pi IZ - \alpha I \\[2mm] \dfrac{dV}{dt} \geq -\eta V \\[2mm] \dfrac{dZ}{dt} \geq -\sigma VZ - \gamma Z \\[2mm] \dfrac{dW}{dt} \geq -\rho W \end{array}\right\} \tag{6}$$

With the basic differential equations methods, the inequalities (6) can be solved to produce:

$$U(t) \geq \exp\left(-\alpha t - \beta \int_0^t V(s)ds\right) \geq 0,$$

$$I(t) \geq \exp\left(-\alpha t - \pi \int_0^t Z(s)ds\right) \geq 0$$

$$V(t) \geq \exp(-\eta t) \geq 0$$

$$Z(t) \geq \exp\left(-\gamma t - \sigma \int_0^t V(s)ds\right) \geq 0$$

and $W(t) \geq \exp(-\rho t) \geq 0$.

Thus, $U(t)$, $I(t)$, $V(t)$, $Z(t)$ and $W(t)$ will be positive in R_+^5, $\forall t \in [0, t_0]$.

Invariant regions

Lemma 2: *All feasible solutions of the EBOV model system* $(1)-(5)$ *are contained in a uniformly bounded region* $\Omega \subset R_+^5$, $\forall t \geq 0$, *where*

$$\Omega = P \cup V \cup Z \cup W \in R_+^2 \times R_+^1 \times R_+^1 \times R_+^1.$$

Proof: At this point, it is required to determine the invariant (bounded) region Ω that contains all feasible populations, the process requires determining the invariant region that contains solutions for each population.

Target cells population

Here, it is required to determine the bounded region that comprises all feasible solutions for the target cells population. Let $\Lambda_P = (U, I) \in R_+^2$ be the solution with initial conditions U_0 and I_0, $\forall t \geq 0$, where P represents total population of the target cells at time t. This is accomplished as follows:

The total population, P is given by

$$P(t) = U(t) + I(t), \forall t \geq 0.$$

This implies that

$$\frac{dP}{dt} = \frac{dU}{dt} + \frac{dI}{dt} \tag{7}$$

Substitution of equations (1) and (2) into (7) produces

$$\frac{dP}{dt} = \Pi - \pi I Z - \alpha P \tag{8}$$

Placing an upper bound on (8) produces

$$\frac{dP}{dt} \leq \Pi - \alpha P \tag{9}$$

Using the basic differential equations methods, the inequality (9) can be solved to produce:

$$P(t) \leq \frac{\Pi}{\alpha} + \left(P_0 - \frac{\Pi}{\alpha} \right) \exp(-\alpha t) \tag{10}$$

where P_0 denotes the initial size of target cells population evaluated at the initial conditions $U_0 \geq 0$ and $I_0 \geq 0$.

Analysis of inequality (10) is achieved with two cases at $t \geq 0$.

Case 1: If $P_0 > \Pi/\alpha$, the largest value of $\frac{\Pi}{\alpha} + \left(P_0 - \frac{\Pi}{\alpha} \right) \exp(-\alpha t)$ is P_0, which is got at $t = 0$. Thus, the inequality (10) reduces to $P(t) \leq P_0$.

Case 2: If $P_0 < \Pi/\alpha$, the value of $\left(P_0 - \frac{\Pi}{\alpha} \right) \exp(-\alpha t)$ is negative and tends to zero as $t \to \infty$. So, the largest value of $P(t) \leq \frac{\Pi}{\alpha} + \left(P_0 - \frac{\Pi}{\alpha} \right) \exp(-\alpha t)$ is Π/α. Thus, $P(t) \leq \Pi/\alpha$. This implies that $P(t) \leq \max\{ P_0, P^* \}$ for all $t \geq 0$ and any value of P_0, where $P^* = \Pi/\alpha$. Thus, $P(t)$ is bounded above. This means all feasible solutions for the target cells population are contained in the region Λ_P defined by

$$\Lambda_P = \left\{ (U, I) \in R_+^2 : P(t) \leq P^* \right\}, \forall t \geq 0. \tag{11}$$

The feasible region Λ_P is upper-bounded for which P^* is an upper bound.

Ebola virus population

At this point, it is required to determine the bounded region consisting of all feasible solutions for the Ebola virus population. Let $\Lambda_V = Z \in R_+^1$ be the solution with initial condition $V_0, \forall t \geq 0$, where V_0 represents total population of EBOV at time t. This is achieved as follows:

Combining Equation 3 and (11) produces the following inequality

$$\frac{dV}{dt} \le \omega P^* - \mu VW - \eta V$$

This can be reduced to

$$\frac{dV}{dt} \le \omega P^* - \eta V \tag{12}$$

Using the basic differential equations methods, the general solution of the inequality (12) is

$$V(t) \le \frac{\omega P^*}{\eta} + \left(V_0 - \frac{\omega P^*}{\eta}\right)\exp(-\eta t) \tag{13}$$

where V_0 is the initial size of Ebola virus population.

Analysis of inequality (13) is achieved with two cases at $t \ge 0$ as follows:

Case 1: If $V_0 > \omega P^*/\eta$, the largest value of $\frac{\omega P^*}{\eta} + \left(V_0 - \frac{\omega P^*}{\eta}\right)\exp(-\eta t)$ is V_0,

which is found at $t = 0$. Thus, the inequality (13) reduces to $V(t) \le V_0$.

Case 2: If $V_0 < \omega P^*/\eta$, the value of $\left(V_0 - \frac{\omega P^*}{\eta}\right)\exp(-\eta t)$ is negative, which

approaches zero as $t \to \infty$. So, the largest value of $\frac{\omega P^*}{\eta} + \left(V_0 - \frac{\omega P^*}{\eta}\right)\exp(-\eta t)$ is

$\omega P^*/\eta$. Thus, $V(t) \le \omega P^*/\eta$. This implies that $V(t) \le \max\{V_0, V^*\}$, $\forall t \ge 0$ and

whatever value of V_0, where $V^* = \omega P^*/\eta$. Consequently, $V(t)$ is bounded above.

This means all feasible solutions for the virus population are contained in the region Λ_V, which is defined by

$$\Lambda_V = \left\{V \in R_+^1 : V(t) \le V^*\right\}, \ \forall t \ge 0. \tag{14}$$

The feasible region Λ_V is upper-bounded for which V^* is an upper bound.

Cytotoxic T Lymphocytes population

Here, it is required to determine the bounded region consisting of all feasible solutions for the CTLs population. Let $\Lambda_Z = Z \in R_+^1$ be the solution with initial condition Z_0, $\forall t \ge 0$, where Z_0 represents total population of CTLs at time *t*. This is achieved as follows:

Combining Equation 4, (11) and (14) produces the following inequality

$$\frac{dZ}{dt} \le \lambda I^* Z - \sigma V^* Z - \gamma Z$$

This can be expressed as

$$\frac{dZ}{dt} \leq (\lambda I^* - \sigma V^* - \gamma)Z \tag{15}$$

Using the basic differential equations methods, the general solution of the inequality (15) is

$$Z(t) \leq Z_0 \exp[(\lambda I^* - \sigma V^* - \gamma)t] \tag{16}$$

Where Z_0 is the initial size of cytotoxic T lymphocytes population.

Analysis of (16) shows that $Z(t)$ is bounded above if and only if

$$\lambda I^* - \sigma V^* - \gamma \leq 0, \ \forall t \geq 0. \text{ So, } Z(t) \leq Z_0.$$

Therefore, all feasible solutions for the cytotoxic T lymphocytes population are contained in the region Λ_Z, which is defined by

$$\Lambda_Z = \{Z \in R_+^1 : Z(t) \leq Z_0\} \tag{17}$$

The feasible region Λ_Z is upper-bounded for which Z_0 is an upper bound.

Antibody cells population

Here, it is required to determine the bounded region comprising all feasible solutions for the antibody cells population. Let $\Lambda_W = W \in R_+^1$ be the solution with initial condition $W_0, \forall t \geq 0$, where W_0 represents total population of the antibody cells at time t. This is achieved as follows:

Combining Equation 5 and (14) produces the following inequality

$$\frac{dW}{dt} \leq \varepsilon V^* W - \rho W$$

This can be expressed as

$$\frac{dW}{dt} \leq (\varepsilon V^* - \rho)W \tag{18}$$

Using the basic differential equations methods, the general solution of the inequality (18) is

$$W(t) \leq W_0 \exp[(\varepsilon V^* - \rho)t] \tag{19}$$

Analysis of the inequality (19) shows that $W(t)$ is bounded above only if $\varepsilon V^* - \rho \leq 0$. Thus, $W(t) \leq W_0$, where W_0 is the initial size of antibody cells population. Therefore, all feasible solutions for the antibody cells population are contained in the region Λ_W, which is defined by

$$\Lambda_W = \{W \in R_+^1 : W(t) \leq W_0\} \tag{20}$$

The feasible region Λ_W is upper-bounded for which W_0 is an upper bound.

Thus, using the results (11), (14), (17) and (20), the invariant (bounded) region, Ω containing all feasible solutions for the whole model system $(1) - (5)$ is

$\Omega = \Lambda_P \times \Lambda_V \times \Lambda_Z \times \Lambda_W = \{P \cup V \cup Z \cup W \in R_+^2 \times R_+^1 \times R_+^1 \times R_+^1\}$, where

$$\Lambda_P = \left\{(U, I) \in R_+^2 : P(t) \le P^*\right\}$$
$$\Lambda_V = \left\{V \in R_+^1 : V(t) \le V^*\right\}$$
$$\Lambda_Z = \{Z \in R_+^1 : Z(t) \le Z_0\}$$

and
$$\Lambda_W = \{W \in R_+^1 : W(t) \le W_0\}$$

Following proven positivity of the state variables $\{U, I, V, Z, W\}$ and invariant (bounded) region Ω for the model system $(1) - (5)$, the proposed EBOV model is mathematically and biologically realistic (Hethcote, 2000). Therefore, it can be employed to investigate the dynamics of EBOV infection in vivo.

Existence of model equilibria

At this point, we examine the existence of disease-free equilibrium E_0 and endemic equilibrium E^*. The equilibria E_0 and E^* are obtained by equating the derivatives (with respect to time) of the variables of the model system $(1) - (5)$ to zero (Mlay *et al.*, 2022; Kung'aro, 2016). More precisely, the equilibria are obtained when $\frac{dU}{dt} = \frac{dI}{dt} = \frac{dV}{dt} = \frac{dZ}{dt} = \frac{dW}{dt} = 0$. Thus, the model equations become

$$\left.\begin{array}{l} \Pi - \beta VU - \alpha U = 0 \\ \beta VU - \pi IZ - \alpha I = 0 \\ \omega I - \mu VW - \eta V = 0 \\ \lambda IZ - \sigma VZ - \gamma Z = 0 \\ \varepsilon VW - \rho W = 0 \end{array}\right\} \tag{21}$$

Solving the equations of the system (21) produces

$$E_0 = (U^*, I^*, V^*, Z^*) = (\Pi/\alpha, 0, 0, 0, 0) \tag{22}$$

and

$$E^* = (U^*, I^*, V^*, Z^*), \tag{23}$$

where $U^* = \dfrac{\Pi\varepsilon}{\beta\rho + \varepsilon}$, $I^* = \dfrac{\sigma\rho + \varepsilon\gamma}{\lambda\varepsilon}$, $V^* = \dfrac{\rho}{\varepsilon}$, $Z^* = \dfrac{\Pi\lambda\varepsilon(\beta\rho + \varepsilon(1-\alpha))}{\pi(\beta\rho + \varepsilon)(\sigma\rho + \varepsilon\gamma)}$ and

$W^* = \dfrac{\omega(\sigma\rho + \varepsilon\gamma) + \lambda\pi\rho}{\lambda\mu\rho}$.

Basic reproduction number

The basic reproduction number is a threshold value that governs the transmission dynamics of an infectious disease within a community or an infected individual, usually represented by R_0. It is greatly instrumental in modeling infectious diseases

(Diekmann *et al*., 1990; Diekmann, 2000), where it is used as a metric to describe the course of infection. If, $R_0 > 1$, the disease is prevalent in the community or infected host; the disease disappears if $R_0 < 1$. It is usually computed using the next generation matrix operator (Tilahun *et al*., 2017*a*; Osman *et al*., 2020*a*; Osman *et al*., 2020*b*). Thus, considering the current Ebola virus dynamics model, R_0 is obtained as follows.

To achieve this, equations (2) and (3) are considered, which are

$$\frac{dI}{dt} = \beta VU - \pi dZ - \alpha I \text{ and } \frac{dV}{dt} = \omega I - \mu VW - \eta V$$

Let M be the next generation matrix defined by $M = FY^{-1}$, where

$$FY^{-1} = \left[\frac{\partial F_i(E_0)}{\partial X_j}\right]\left[\frac{\partial Y_i(E_0)}{\partial X_j}\right]^{-1}. \tag{24}$$

Let $F_i = \begin{bmatrix} f_1 & f_2 \end{bmatrix}^T$ and $Y_i = \begin{bmatrix} y_1 & y_2 \end{bmatrix}^T$. Then $F_i = \begin{bmatrix} \beta VU & \omega I \end{bmatrix}^T$ and

$$Y_i = \begin{bmatrix} \pi dZ + \alpha I & \mu VW + \eta V \end{bmatrix}^T$$

This implies that

$$\left[\frac{\partial F_i}{\partial X_j}\right] = \begin{bmatrix} \frac{\partial f_1}{dI} & \frac{\partial f_1}{\partial V} \\ \frac{\partial f_2}{\partial I} & \frac{\partial f_2}{\partial V} \end{bmatrix} = \begin{bmatrix} 0 & \beta U \\ \omega & 0 \end{bmatrix},$$

$$F = \left[\frac{\partial F_i(E_0)}{\partial X_j}\right] = \begin{bmatrix} 0 & \frac{\beta \Pi}{\alpha} \\ \omega & 0 \end{bmatrix} \tag{25}$$

$$\left[\frac{\partial Y_i}{\partial X_j}\right] = \begin{bmatrix} \frac{\partial y_1}{dI} & \frac{\partial y_1}{\partial V} \\ \frac{\partial y_2}{\partial I} & \frac{\partial y_2}{\partial V} \end{bmatrix} = \begin{bmatrix} \pi Z + \alpha & 0 \\ 0 & \eta \end{bmatrix},$$

$$Y = \left[\frac{\partial Y_i(E_0)}{\partial X_j}\right] = \begin{bmatrix} \alpha & 0 \\ 0 & \eta \end{bmatrix},$$

$$Y^{-1} = \begin{bmatrix} \frac{1}{\alpha} & 0 \\ 0 & \frac{1}{\eta} \end{bmatrix} \tag{26}$$

And then substituting (25) and (26) into (24) produces M. Thus, M is given by

$$M = FY^{-1} = \begin{bmatrix} 0 & \dfrac{\beta\Pi}{\alpha} \\ \omega & 0 \end{bmatrix} \begin{bmatrix} \dfrac{1}{\alpha} & 0 \\ 0 & \dfrac{1}{\eta} \end{bmatrix} = \begin{bmatrix} 0 & \dfrac{\beta\Pi}{\alpha\eta} \\ \dfrac{\omega}{\alpha} & 0 \end{bmatrix}.$$

The eigenvalues of M are given by $|\lambda I - M| = |\lambda I - FY^{-1}| = 0$,

where $\lambda I - M = \begin{bmatrix} \lambda & 0 \\ 0 & \lambda \end{bmatrix} - \begin{bmatrix} 0 & \dfrac{\beta\Pi}{\alpha\eta} \\ \dfrac{\omega}{\alpha} & 0 \end{bmatrix} = \begin{bmatrix} \lambda & -\dfrac{\beta\Pi}{\alpha\eta} \\ -\dfrac{\omega}{\alpha} & \lambda \end{bmatrix}.$

Thus,

$$|\lambda I - FY^{-1}| = 0 \Rightarrow \begin{vmatrix} \lambda & -\dfrac{\beta\Pi}{\alpha\eta} \\ -\dfrac{\omega}{\alpha} & \lambda \end{vmatrix} = 0 \tag{27}$$

From (27), the eigenvalues of M are

$$\lambda_1 = \sqrt{\dfrac{\omega\beta\Pi}{\alpha^2\eta}} \text{ and } \lambda_2 = -\sqrt{\dfrac{\omega\beta\Pi}{\alpha^2\eta}}$$

The basic reproduction number, R_0 is the spectral radius of the next generation matrix M, which is the dominant eigenvalue (Van de Driessche and Watmough, 2002). That is, $R_0 = \rho(M) = \sqrt{\dfrac{\omega\beta\Pi}{\alpha^2\eta}}$.

Consequently, the basic reproduction number, R_0 is

$$R_0 = \sqrt{\dfrac{\omega\beta\Pi}{\alpha^2\eta}} \tag{28}$$

The threshold parameter R_0 governs the course of Ebola virus infection in an infected host. It merely depends on the parameters for replication rate of the virus, infection rate, increasing rate of uninfected target cells, natural death rate of target cells and natural death rate of the virus. On the other hand, the immune system does not influence R_0 as it encompasses no any parameters affiliated to the cytotoxic T lymphocytes and antibody cells populations.

Stability analysis of the model equilibria

Global stability of disease-free equilibrium point
In this section, we analyze global stability of disease-free equilibrium point using Metzler matrix method as detailed by Castillo-Chaves *et al.* (2002) and applied by Kamgang and Sallet (2008); Dumont *et al.* (2008); Kung'aro (2016); Ngeleja (2019)

and Ismail (2021). To achieve this, we initially apportion the model system of equations $(1)-(5)$ into transmitting and non-transmitting components.

Let Y_n be the vector for non-transmitting compartments; Y_i be the vector for transmitting compartments and $Y_{DFE,n}$ be the vector of disease-free equilibrium point. Then

$$\begin{cases} \dfrac{dY_n}{dt} = C_1\left(Y_n - Y_{DFE,n}\right) + C_3 Y_i \\ \dfrac{dY_i}{dt} = C_2 Y_i \end{cases} \tag{29}$$

Thus, we have $Y_n = (U, Z, W)^T$, $Y_i = (I, Z)^T$, $Y_{DFE,n} = \left(\dfrac{\Pi}{\alpha}, 0, 0\right)$ and

$$Y_n - Y_{DFE,n} = \begin{pmatrix} U - \dfrac{\Pi}{\alpha} \\ Z \\ W \end{pmatrix} \qquad .$$

Thus, the equations of the system (29) become

$$\begin{bmatrix} \Pi - \beta UV - \alpha U \\ \lambda IZ - \sigma VZ - \gamma Z \\ \varepsilon VW - \rho W \end{bmatrix} = C_1 \begin{bmatrix} U - \dfrac{\Pi}{\alpha} \\ Z \\ W \end{bmatrix} + C_3 \begin{bmatrix} I \\ V \end{bmatrix} \tag{30}$$

and

$$\begin{bmatrix} \beta UV - \pi IZ - \alpha I \\ \omega I - \mu VW - \eta V \end{bmatrix} = C_2 \begin{bmatrix} I \\ V \end{bmatrix} \tag{31}$$

From (30) and (31), we deduce that

$$C_1 = \begin{bmatrix} -\alpha & 0 & 0 \\ 0 & -\gamma & 0 \\ 0 & 0 & -\rho \end{bmatrix}, \quad C_2 = \begin{bmatrix} -\alpha & \dfrac{\beta \Pi}{\alpha} \\ \omega & -\eta \end{bmatrix} \text{ and } C_3 = \begin{bmatrix} 0 & -\dfrac{\beta \Pi}{\alpha} \\ 0 & 0 \\ 0 & 0 \end{bmatrix}.$$

The eigenvalues of the matrix C_1 are $-\alpha$, $-\gamma$ and $-\rho$, which are real and negative. Thus, the results ratify that the system

$$\frac{dY_n}{dt} = C_1(Y_n - Y_{DFE,n}) + C_3 Y_i.$$

is globally asymptotically stable at $Y_{DFE,n}$. Besides, we find that the matrix C_2 contains negative main diagonal and non-negative off-diagonal elements. Therefore, C_2 is a stable Metzler matrix. Hence, the disease-free equilibrium E_0 is globally asymptotically stable when $R_0 < 1$. Theorem 1 summarizes the results.

Theorem 1: *The disease-free equilibrium, E_0 of the Ebola virus infection model system $(1) - (5)$ is globally asymptotically stable if $R_0 < 1$.*

Global stability of endemic equilibrium point

In this section, we analyze global stability of the endemic equilibrium (E_0) using the approach of Van den Driessche and Watmough (2002), Korobeinikov (2004), McCluskey (2006); Mpeshe *et al.* (2011); Ullah *et al.* (2013), Kung'aro (2016) and Ngeleja (2019). The analysis is done using an appropriate Lyapunov function constructed from the model system $(1) - (5)$.

We construct the Lyapunov function of the form

$$L = \sum b_i (x_i - x_i^* \ln x_i), \tag{32}$$

where b_i connotes a properly selected positive constant $b_i > 0$, x_i stands for the population of the ith compartment and x_i^* defines the equilibrium point, which is the E_0 in this case.

Thus, using the Lyapunov function form (32), we have

$$L = b_1(U - U^* \ln U) + b_2(I - I^* \ln I) + b_3(V - V^* \ln V) + b_4(Z - Z^* \ln Z) . + b_5(W - W^* \ln W) \tag{33}$$

At this point, the constants $b_i(1,2,...,5)$ are non-negative in Ω. The Lyapunov function L and its constants $b_i(1,2,...,5)$ are suitably selected such that L is continuous and differentiable in a space.

Differentiating (33) with respect to time *t* produces

$$\frac{dL}{dt} = b_1\left[1 - \frac{U^*}{U}\right]\frac{dU}{dt} + b_2\left[1 - \frac{I^*}{I}\right]\frac{dI}{dt} + b_3\left[1 - \frac{V^*}{V}\right]\frac{dV}{dt} + b_4\left[1 - \frac{Z^*}{Z}\right]\frac{dZ}{dt} + b_5\left[1 - \frac{W^*}{W}\right]\frac{dW}{dt}$$

$$= b_1\left(1 - \frac{U^*}{U}\right)[\Pi - \beta UV - \alpha U] + b_2\left(1 - \frac{I^*}{I}\right)[\beta UV - \pi I Z - \alpha I] + b_3\left(1 - \frac{V^*}{V}\right)[\omega I - \mu VW - \eta V]$$

$$+ b_4\left(1 - \frac{Z^*}{Z}\right)[\lambda I Z - \sigma VZ - \gamma Z] + b_5\left(1 - \frac{W^*}{W}\right)[\varepsilon VW - \rho W] \tag{34}$$

At the endemic equilibrium point, E^*, (34) becomes

$$\frac{dL}{dt} = b_1\left(1 - \frac{U^*}{U}\right)[\Pi - \beta V^* U^* - \alpha U^*] + b_2\left(1 - \frac{I^*}{I}\right)[\beta V^* U^* - \pi I^* Z^* - \alpha I^*]$$

$$+ b_3\left(1 - \frac{V^*}{V}\right)\left[\omega I^* - \mu V^* W^* - \eta V^*\right] + b_4\left(1 - \frac{Z^*}{Z}\right)\left[\lambda I^* Z^* - \sigma V^* Z^* - \gamma Z^*\right]$$

$$+ b_5\left(1 - \frac{W^*}{W}\right)\left[\varepsilon V^* W^* - \rho W^*\right] \tag{35}$$

Simplification of (35) produces

$$\frac{dL}{dt} = -b_1\left(1 - \frac{U^*}{U}\right)^2 - b_2\left(1 - \frac{I^*}{I}\right)^2 - b_3\left(1 - \frac{V^*}{V}\right)^2 - b_4\left(1 - \frac{Z^*}{Z}\right)^2 - b_5\left(1 - \frac{W^*}{W}\right)^2 + G(U,I,V,Z,W)$$

where the function $G(U,I,V,Z,W)$ is non-positive.

Using the approach of Mukandavire *et al.* (2009); Kung'aro (2016) and Ngeleja (2019), we find that $G \leq 0$ for all $G(U,I,V,Z,W)$. Therefore, $\frac{dL}{dt} \leq 0$ for all $U,I,V,Z,W > 0$ and is zero when $U = U^*$, $I = I^*$, $V = V^*$, $Z = Z^*$ and $W = W^*$. Hence, the largest compact invariant set in Ω, such that $\frac{dL}{dt} = 0$, is the singleton E^*, which represents the endemic equilibrium point of the model system $(1) - (5)$. LaSalle's Invariant Principle (LaSalle, 1976) guarantees that E^* is globally asymptotically stable in $\overset{0}{\Omega}$, the interior of Ω. Theorem 2 summarizes the results.

Theorem 2: *If* $R_0 > 1$ *then the Ebola virus infection model system* $(1) - (5)$ *has a unique endemic equilibrium point and is globally asymptotically stable in the interior of the region* Ω.

Sensitivity analysis

Sensitivity analysis aims at analyzing the model parameters in order to determine parameters that have enormous transmission influence on the disease (Muia *et al*., 2018; Osman *et al*., 2020*d*). The analysis considers the parameters embedded in R_0 because these are the contributing factors of disease spread or extinction. This can be known by the sensitivity index of each parameter. As stated by Chitnis *et al* (2008), the sensitivity index of each parameter is computed using the relation:

$$S_Q^{R_0} = \frac{Q}{R_0} \times \frac{\partial R_0}{\partial Q} \tag{36}$$

where Q is the parameter to be analyzed and $S_Q^{R_0}$ is the sensitivity index of parameter Q. If $S_Q^{R_0} < 0$, the parameter Q has an effect of controlling the disease; but then if $S_P^{R_0} > 0$, Q has an effect of increasing the disease spread (Onsongo *et al*., 2022). Then the sensitivity indices of the parameters embedded in R_0 are computed

using relation (36) and parameter values itemized in Table 2. Most parameters values are adopted from different literatures and others are just estimated values.

Table 2. Parameter values used for sensitivity analysis.

Parameter	Parameter value	Units	Source
β	0.1	$mil \times cell^{-1} \times day^{-1}$	CDC (2014).
α	0.5	$cell \times day^{-1}$	Ismail and Mtunya (2021).
γ	0.5	$cell \times day^{-1}$	Wester (2015).
η	1.15	$cell \times day^{-1}$	Nguyen *et al*. (2015).
ρ	1.05	$cell \times day^{-1}$	Estimated.
μ	1.03	$mil \times cell^{-1} \times day^{-1}$	Estimated.
ε	0.05	$mil \times cell^{-1} \times day^{-1}$	Estimated.
ω	40.9	$cell \times day^{-1}$	Wester (2015).
λ	0.1	$mil \times cell^{-1} \times day^{-1}$	Banton *et al*. (2010).
π	0.1	$mil \times cell^{-1} \times day^{-1}$	Wester (2015).
σ	0.1	$mil \times cell^{-1} \times day^{-1}$	Ismail and Mtunya (2021).
Π	5.05	$cell \times mil^{-1} \times day^{-1}$	Wester (2015).

The sensitivity indices of all parameters are computed and their values are altogether itemized in Table 3. Therefore, $S_{\omega}^{R_0} = \dfrac{\omega}{R_0} \times \dfrac{\partial R_0}{\partial \omega} = 0.1036$, $S_{\beta}^{R_0} = \dfrac{\beta}{R_0} \times \dfrac{\partial R_0}{\partial \beta} = 42.380$ and so on.

Table 3. Sensitivity indices of the model parameters embedded in R_0

Parameter	Sensitivity index
ω	+0.1036
Π	+0.8392
η	-3.6850
α	-16.952
β	+42.380

The sensitivity indices in Table 3 are listed in increasing magnitude of their absolute values from above.

Numerical simulations

In mathematical modeling of infectious diseases dynamics, numerical simulations are usually performed to substantiate analytical results of formulated models (Ismail and Luboobi, 2019; Ismail and Mtunya, 2021; Sakkoum *et al*., 2022). Basically,

numerical simulations are employed to investigate dynamical behaviors of model systems whose mathematical equations are too complicated to provide analytical solutions (Tilahun *et al.*, 2017*b*; Osman *et al*., 2018*c*; Otoo *et al*., 2021). Considering the current model system $(1) - (5)$, numerical simulations are performed to validate the analytical results. This is achieved using the parameter values itemized in Table 2. However, two sets of values for the parameters embedded in the basic reproduction number, R_0, are appropriately selected in such a way that one set constitute $R_0 < 1$ and the other, $R_0 > 1$ to study numerically the existence of disease-free and endemic equilibria respectively.
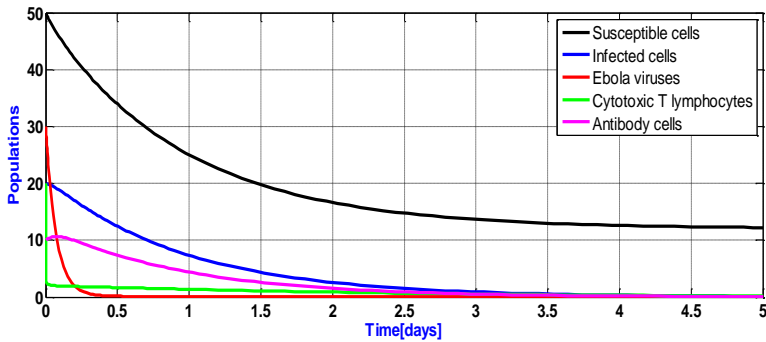
(a)
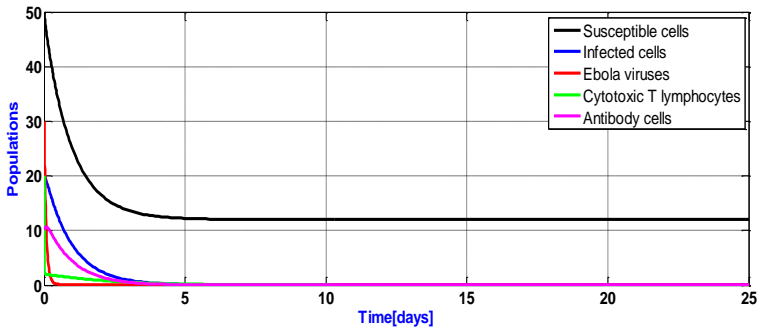
(b)

Figure 2 (a) and (b). Simulations for solution trajectories showing the disease-free point, obtained using the parameter values $\Pi = 12.5$, $\beta = 0.01$, $\alpha = 1.04$, $\omega = 0.09$ and $\eta = 3.15$; and initial conditions $S_0 = 50$, $I_0 = 20$, $V_0 = 30$, $Z_0 = 20$ and $W_0 = 10$. In this case, $R_0 = 0.5746$.
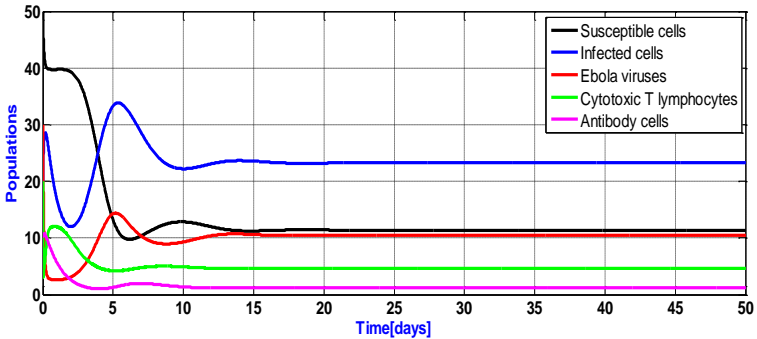
Figure 3. Simulations for solution trajectories showing the endemic point, obtained using the parameter values $\Pi = 12.5$, $\beta = 0.1$, $\alpha = 0.05$, $\omega = 1.09$ and $\eta = 1.15$; and initial conditions $S_0 = 50$, $I_0 = 20$, $V_0 = 30$, $Z_0 = 20$ and $W_0 = 10$. In this case, $R_0 = 21.7695$.
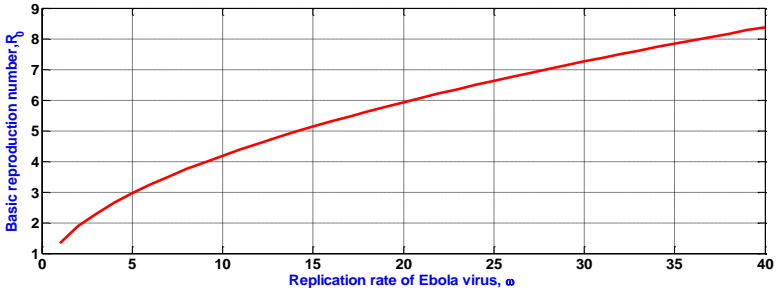

Figure 4. Simulation of the effect of replication rate of the virus on R_0.

Figure 5. Simulation of the effect of infection rate on R_0.

Figure 6: Simulation of the effect of production rate of uninfected target cells on R_0.
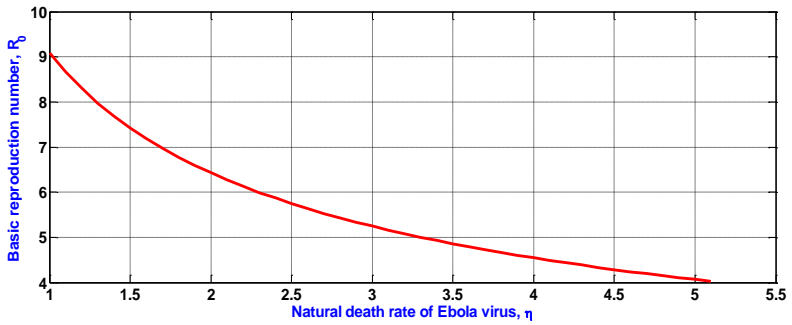
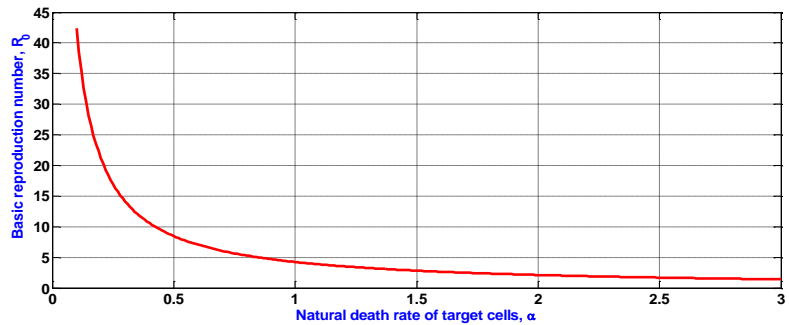Figure 7. Simulation of the effect of natural death rate of the virus on R_0.

Figure 8. Simulation of the effect of natural death rate of target cells on R_0.
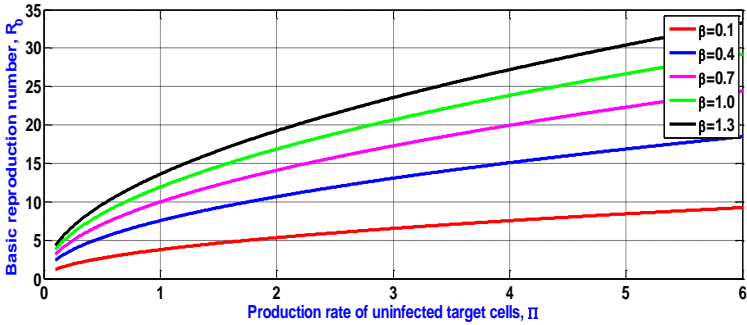
Figure 9. Simulation of the effect of production rate of uninfected target cells on R_0 with various infection rates.
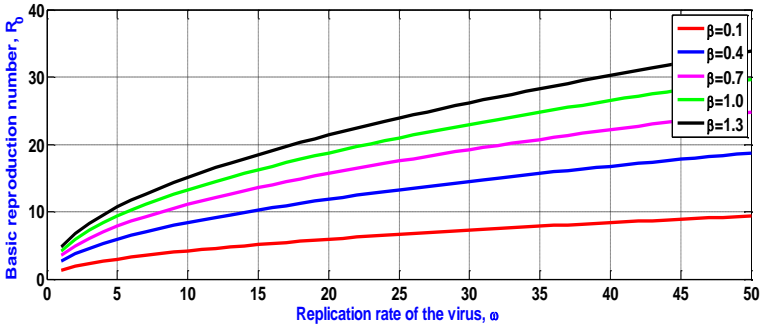

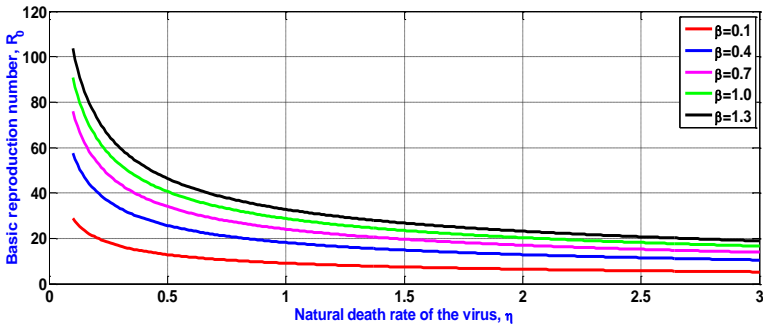Figure 10. Simulation of the effect of virus replication rate on R_0 with various infection rates.

Figure 11. Simulation of the effect of natural death rate of the virus on R_0 with various infection rates.
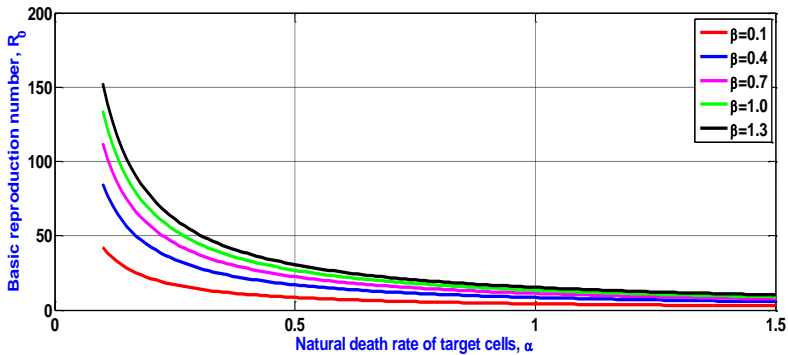
Figure 12. Simulation of the effect of natural death rate of target cells on R_0 with various infection rates.

RESULTS AND DISCUSSION

This study aimed to investigate the dynamics of Ebola virus infection in vivo through modeling. This was achieved through stability analysis of the model equilibria and sensitivity analysis of the basic reproduction number, R_0 with respect to the model parameters. Analytically, the results show that the basic reproduction number R_0 does not comprise parameters linked to the immune system, implying that the CTLs and antibody responses do not determine the course of EVD in vivo.

The global stability analysis of the model equilibria indicate that the disease-free equilibrium point is asymptotically stable if $R_0 < 1$, which implies that the disease can eventually disappear as time t elapses to infinity $(t \to \infty)$. Analysis of the endemic equilibrium point established asymptotic stability if $R_0 > 1$, which implies that the disease can persist within the host. The sensitivity indices presented in Table 3 indicate that R_0 increases as the parameters ω, Π and β increase and vice versa. This is reflected by the parameters' positive sensitivity indices. It is also observe that R_0 decreases with increasing parameters η and α, and vice versa, which is reflected by the parameters' negative sensitivity indices. Specifically, an increase in the infection rate by 10% would increase the basic reproduction number by 423.8%. Furthermore, increasing the natural death rates of uninfected target and infected cells by 10% would decrease R_0 by 169.52%. Biologically, this implies the disease spread increases as R_0 increases and vice versa. That is, at greater values of R_0 the disease is prevalent and it disappears at smaller values of R_0. The parameters with the

greatest absolute values of sensitivity indices would ether decrease or reduce the spread of the disease at faster paces.

Numerical simulations were implemented to illustrate the stability of the model equilibria and the influence of the parameters on the basic reproduction number R_0.

Figures 2*a* and 2*b* (Figure 2*a* zoomed to Figure 2*b*) illustrate the existence of disease-free equilibrium (DFE) defined by the DFE point, where the trajectories corresponding to the infected, virus, CTLs and antibody cells populations converge to zero as $t \rightarrow \infty$. The trajectory corresponding to the uninfected target cells population converges to a no-zero value. Overall, this means that the state of no infection can be attained after some time. On the other hand, Figure 3 illustrate the existence of endemic equilibrium (EE) defined by the EE point, where it is observed that all trajectories corresponding to the populations converge to a non-zero value as time elapses to infinity. This implies that the disease can persist in the host in the absence of intervention.

Graphs in Figures 4, 5 and 6 illustrate that the basic reproduction number, R_0 increases as the replication rate of the virus, ω; infection rate, β and production rate of uninfected target cells, Π increase respectively and vice versa. Biologically, this means the EBOV infection prevails whenever the values of ω, Π and β are increased. On the other hand, Figures 7 and 8 illustrate that R_0 decreases with increase in the natural death rate of the virus, η and natural death rate of target cells, α respectively and vice versa. This implies α and η reduce the spread of infection whenever their values are increased.

Graphs in Figures 9 and 10 still show that R_0 increases as the values of ω, Π and β increase; but as they increase infinitely, R_0 increases drastically due to double effects. On the other hand, plots in Figures 11 and 12 show that as η and α increase R_0 decreases and it increases as β increases. But, one important information portrayed in Figures 11 and 12 is that η and α mostly influence R_0 as they increase substantially. This means the effect of β on R_0 is immaterial at higher values of η and α. Consequently, the parameter for the infection rate, β, being the most sensitive one, can be employed to decrease R_0. Decreasing β will decrease R_0 as well. (Figures 9, 10, 11 and 12). Absolutely, this will reduce the spread of infection in vivo.

CONCLUSION AND RECOMMENDATIONS

This paper presents a deterministic mathematical model proposed to investigate the dynamics of EBOV. A detailed analysis of the model was implemented to determine the invariant region and establish positivity of the solutions set of the model system; obtain equilibrium points, basic reproduction number, R_0. Global stability analysis of the equilibrium points and sensitivity analysis of the model parameters rooted in R_0 were implemented. Numerical simulations were done to portray existence of the model equilibria and variations of R_0 with respect to the model parameters linked to R_0. Based on the analytical results and observations, it was shown that the model is mathematically and biologically well posed, which implies that the model can be used to effectively investigate the dynamics of EBOV in vivo. The results also showed that the disease-free and endemic equilibrium points are globally asymptotically stable, suggesting that strategic control measures can be taken to eradicate the disease. The sensitivity indices of the model parameters imbedded in R_0 portrayed that the parameters for the infection rate, production rate of uninfected target cells and virus replication rate are positively sensitive while the parameters for natural death rate of target cells and the natural death rate of the virus are negatively sensitive. It is further shown that the parameter for the infection rate is the most sensitive one whereas the parameter for the virus replication rate is the least sensitive one. This implies that the parameter for the infection rate is highly influential to R_0 while the virus replication rate is slightly influential to R_0. This further implies that decreasing the value of infection rate will significantly decrease the value of R_0 and so the number of secondary infections will decrease enormously. Consequently, the most influential parameters can be considered for the disease control. The results suggest implementation of deliberate control measures to eradicate EBOV disease by considering sites in the model to which the most sensitive parameters are affiliated.

ACKNOWLEDGEMENTS

CONFLICT OF INTEREST

I declare that there is no conflict of interest whatsoever.

REFERENCES

Banton, S., Roth, Z and Pavlovic., M. (2010). Mathematical modeling of ebola virus dynamics as a step towards rational vaccine design. In: 26th Southern Biomedical Engineering Conference (SBEC), April 30-May 2, 2010, pp 196-200, College Park, Maryland, USA.

Beeching, N.I., Fenech, M and Houliham, C.F. (2014). Ebola virus disease. *BMJ: Clinical Review* **349**: g7348.

CDC (2014). Ebola virus disease. *CDC Report* **63**(50): 1199–1201.

Chitnis, N., Hyman, J.M and Cushing, J.M. (2008). Deterrmining importants parameters in the spread of malaria through the sensitivity analysis of mathematics models. *Bulletin of Mathematical Biology* **70**(5): 1272–1296.

Carter, J and Saunders, V. (2013). Virology: Principle and applications. John Wiley & son, UK.

Castillo-Chvez, C., Blower, S., Driessche, P., Kirschner, D and Yakubu, A.A. (2002). Mathematical approaches for emerging and reemerging infectiuos diseases: Models, methods and theory. *Springer.*

Diekmann, O., Heesterbeek, J.A.P and Metz, J.A.J. (1990). On the definition and the computation of the basic reproductive ratio R_0 in models for infectious diseases in heterogeneous populations. *Journal of Mathematical Biology* **28**(4): 365–382.

Diekmann, O and Heesterbeek, J.A.P. (2000). Mathematical epidemiology of infectious diseases: Model building analysis and interpretation. John Wiley & Son, UK.

Dumont, Y., Chiroleu, F and Domerg, C. (2008). On a tmporal model for the chikungunya disease: modeling, theory and numerics. *Mathematical Biosciences* **213**(1): 80–91.

ECDC (2022). Ebola virus disease. Fact sheet about ebola virus disease, Updated October 2022. https://www.ecdc.europa.eu/en/infectious-disease-topics/z-disease-list/ ebola-virus-disease/ facts / factsheet-about-ebola-disease, (Accessed June 03, 2023).

Eyaran, W.E, Osman, S and Wainaina, M. (2019). Modeling and analysis of SEIR with delay differential equation. *Global Journal of Pure and Applied. Mathematics* **15**(4): 365–382.

Fauci, A.S. (2014). Ebola underscoring the global disparities in health care resources.

Fauci, A.S. (2014). Ebola underscoring the global disparities in health care resources. *New England Journal of Medicine* **371**(12): 1084-1086.

Fritz, E. (2012). Innate immune response to ebola virus infection. https: // www. bdbioscience. com /documents/Grant_E_Fritz, (Accessed September 20,2022).

Hethcote, H.W. (2000). The mathematics of infectious diseases. *SIAM Review* **42**(4): 599–653.

IFRC (2022). DRC: Ebola virus disease outbreak-emergence plan of action (EPoA). *Situation Report.* https://www. reliefweb. Int / democratic-republi-congo/ drc- ebola-virus-disease-outbreak-emergency-plan-action-epoa-dref-n, (Accessed October 12,2022).

Ismail, S and Luboobi, L. (2019). Dyanamics of acute hepetitis c virus subject to responses of cytotoxic T lymphocytes and antibodies. *Journal of Mathematical and Computational Science* **9**(1):102–120.

Ismail, S and Mtunya, A.P. (2021). A mathematical analysis of an in-vivo ebola virus transmission dynamics model. *Tanzania. Journal of Science* **47**(4): 1464–1477.

Kamgang, J.C and Sallet, G. (2008). Computation of threshold conditions for epidemiological models and global stability of disease-free equilibrium DFE. *Mathematical Biosciences* **213**(1):1–12.

Korobeinikov, A. (2004). Lyapunov functions and global properties for SEIR and SEIS epidemic models. *Mathematical Medicine and Biology* **21**(2): 75–83.

Kung'aro, M. (2016). Mathematical modeling of intra and inter dynamics and control of yellow fever in primate and human populations. PhD Thesis, Nelson Mandela Institution of Science and Technology, Arusha, Tanzania.

McCluskey, C. (2006). Lyapunov funtions for tuberculosis models with fast and slow progression. *Mathematical Biosciences and Enineering: MBE* **3**(4): 603–614.

Melinda, R. (2022) Ebola virus infection. https://www.webmd.com/a-to-zguides/ebola-fever-virus-infection#091e9c5e80007fda-2-7, (Accessed September 1,2022).

Mlay, G.M., Hugo, A.K and Kabigi, M.B. (2022). Modeling the impacts of immgrants on COVID-19 transmission dynamics with control measures. *Tanzania Journal of Science* **48**(3): 569–584.

Mpeshe, S.C., Luboobi, L.S and Nkansah-Gyekye, Y. (2014). Modeling the impact of climate change on the dynamics of rift valley fever. *Computational and Mathematical Methods in Medicine* **201**: 1–12.

Mua, D.W., Osman, S and Wainaina, M. (2018). Modeling and analysis of trypanosomiasis transmission mechanism. *Global Journal of Pure and Applied Mathematics* **14**(10): 1311–1331.

Mukandavire, Z. Garira, W and Tchuenche, J. (2009). Modelling effects of public health educational campaighs on HIV/AIDS transmission dynamics. *Applied Mathematical Modeling* **33**(4): 2084–2095.

Ngeleja, R.C. (2019). Mathematical modeling of the effect of seasonal weather variations on the dynamics of plague disease. PhD Thesis, Nelson Mandela Institution of Science and Technology, Arusha, Tanzania.

Nguyen, V.K., Binder, S.C., Boianelli, A., Hermann, M.M and Hernandez-Vargas, E.A. (2015) Ebola virus infection modeling and identifiability problems. *Frontiers in Microbiology* **6**: 1–11.

Nowak, M.A and May, R.M. (2000). Virus dynamics. mathematical principles of immunology and virology, Vol.291. Oxford University Press, UK.

Okosun, K.O and Makinde, O.D. (2014). Optimal control analysis of hepatitis C virus with acute and chronic stages in the presence of treatment and infected immigrants. *International Journal of Biomathematics* **7**(2): 1450019.

Onsongo, W.M., Mwini, E.D., Nyanaro, B.N and Osman, S. (2022). Stability analysis and modelling the dynamics of psittacosis in human and poultry populations. *Communications in Mathematical Biology and Neuroscience* **9**(2022): 1–30.

Osman, S and Makinde, O.D. (2018). A mathematical model for coinfection of listeriosis and anthrax diseases. *International Journal of Mathematics and Mathematical Sciences* **2018**(3): 1–14.

Osman, S., Makinde, O.D. and Theuri, D.M. (2018). Mathematical modeling of transmission dynamics of anthrax in human and animal population. *Mathematical Theory and Modeling* **8**(6): 47–67.

Osman, S., Makinde, O.D., Togbenon, H.A and Otoo, D. (2020a). Mathematical modeling of dynamics of compylobacteriosis using nonstandard finite difference approach with optimal control. *Computational and Mathematical Methods in Medicine* **2020**(2020): 1–12.

Osman, S., Otoo, D and Makinde, O.D. (2020b). Modeling anthrax with optimal control and cost effectiveness analysis. *Applied Mathematics* **11**(3): 255–275.

Osman, S., Otoo, D and Sebil, C. (2020c). Bifurcation, sensitivity and optimal control analysis of modeling anthrax-listeriosis co-dynamics. *Communications in Mathematical Biology and Neuroscience* **2020**(2020): 1–33.

Osman, S., Otoo, D and Sebil, C. (2020d). Analysis of listeriosis transmission dynamics with optimal control. *Applied Maths* **11**(7): 712–737.

Otoo, D., Abeasi, I.O., Osman, S and Donkoh, E.K. (2021). Mathematical modeling and analysis of the dynamics of hepatitis B with optimal control. *Communications in Mathematical Biology and Neuroscience* **2021**(2021): 1–32.

Peters, C.J and LeDuc, J.W. (1999). An introduction to ebola: The virus and the disease. *Journal of Infectious Disease* **179** (Suppl.1): xi–xvi.

Ramirez, I. (2014). Mathematical modeling of immune responses to hepatitis C virus infection. M.Sc. Thesis, East Tennessee State Unversity, US.

Rihan, A.F and Rihman, D.H.A. (2013). Delay differential model for tumor-immune dynamics with HIV infection of CD4+ T cells. *International Journal of Computer Mathematics* **90**(3): 594–614.

Roemer, P.A. (2013). Stochastic modeling of the persistence of HIV: Early population dynamics. Trident Scholar Project Report, no.420, United States Noval Academy, US.

Tilahun, G.T., Makinde, O.D and Malonza, D. (2017a). Modeling and optimal control of pneumonia disease with cost-effective strategies. *Journal of Biological Dynamics* **11**(52): 400–426.

Tilahun, G.T., Makinde, O.D and Malonza, D. (2017b). Modeling and optimal control of typhoid fever disease with cost-effective strategies. *Computational and Mathematical Methods in Medicine* **2017**(2017): 2324518.

Tseng, C.P and Chan, Y.J. (2015). Overview of ebola virus disease in 2014. *Journal of Chinines Medical Association* **78**(1): 51–55.

Ullah, R.; Zaman, G and Islam, S. (2013). Stability analysis of a general SIR epidemic model. *Fast Transactions on Mathematics* **1**(1): 16–20.

Van Den Driessche, P and Watmough, J. (2002). Reproduction numbers and sub-threshold endemic equilibria for compartmental models of disease transmission. *Mathematical Biosciences* **180**(1): 29–48.

Wester, T. (2015). Analysis and simulation of a mathematical model of ebola virus dynamics in vivo. *Society Indian Applied Maths* **8**: 236–256.

Wodarz, D. (2007). Killer cell dynamics: Mathematical and computational approaches to immunology. Springer Verlag, New York, US.

WHO (2021). Ebola outbreak-Democratic Republic of the Congo-North Kivu, Ituri 2018-2020. WHO Health Emergencies List. https://tinyurl.com/22u4bkvy, (Accessed December 10, 2022).

WHO (2022). WHO: Bolster ebola disease outbreak response in Uganda. https://www.afro.who. Int/countries/uganda/news/who-bolster-ebola-outbreak-response-uganda, (Accessed January 27, 2022).